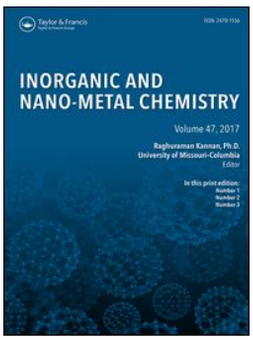

Inorganic and Nano-Metal Chemistry

ISSN: 2470-1556 (Print) 2470-1564 (Online) Journal homepage: https://www.tandfonline.com/loi/lsrt21

Investigation of catalytic, anti-bacterial, anti-oxidant, and DNA cleavage properties of bimetallic and trimetallic magnetic nanoalloys base on cupper

Kaveh Parvanak Boroujeni, Ahmad Farokhnia, Mansooreh Shahrokh & Mohsen Mobini

To cite this article: Kaveh Parvanak Boroujeni, Ahmad Farokhnia, Mansooreh Shahrokh & Mohsen Mobini (2019): Investigation of catalytic, anti-bacterial, anti-oxidant, and DNA cleavage properties of bimetallic and trimetallic magnetic nanoalloys base on cupper, Inorganic and Nano-Metal Chemistry, DOI: 10.1080/24701556.2019.1574818

To link to this article: https://doi.org/10.1080/24701556.2019.1574818

Published online: 11 Apr 2019.

INORGANIC AND NANO-METAL CHEMISTRY
https://doi.org/10.1080/24701556.2019.1574818

Investigation of catalytic, anti-bacterial, anti-oxidant, and DNA cleavage properties of bimetallic and trimetallic magnetic nanoalloys base on cupper

Kaveh Parvanak Boroujeni[a], Ahmad Farokhnia[a], Mansooreh Shahrokh[a], and Mohsen Mobini[b]

[a]Department of Chemistry, Shahrekord University, Shahrekord, Iran; [b]Department of Genetics, Shahrekord University, Shahrekord, Iran

ABSTRACT

Bimetallic and trimetallic magnetic nanoalloys base on cupper were easily prepared from their starting materials. These nanoparticles (NPs) were used for the synthesis of biscoumarines by two-component one-pot domino Knoevenagel-type condensation/Michael reaction between aldehydes and 4-hydroxycoumarin. Also, anti-bacterial, anti-oxidant, and DNA cleavage properties of these NPs were investigated.

ARTICLE HISTORY
Received 24 February 2018
Accepted 2 January 2019

KEYWORDS
Magnetic nanoalloys; nanocatalyst; anti-bacterial activity; anti-oxidant activity; DNA cleavage properties

Introduction

One of the most important aspects of nanotechnology is alloying two or more elements to make nanoalloys with modified properties including high strength, ductility, corrosion resistance, moderate strength, magnetic, high toughness, and electrical and thermal conductivity properties. Among these properties, magnetic behavior is considered as the most important feature of the magnetic nanoalloys.[1] For example, Cu and Ag do not have magnetic properties, but by mixing them with Co or Ni and converting them into bimetallic or trimetallic alloys, they show magnetic properties.[2] On the other hand, sometimes, some of the heterogeneous alloys made of nonmagnetic metals like Cu–Co or Cu–Ni that are used in the structure of sensors, exhibit enhanced magnetoresistance in contrast to the homogeneous single metals like Co or Ni.[3]

Nowadays, the magnetic nanoalloys have been received considerable attention as catalyst for synthetic applications due to their high surface-to-volume ratio and easy separation from reaction vessel via an external magnet and maintaining their catalytic activity after several reaction cycles.[4] For instance, several magnetic catalysts based on Cu alloys have been used as efficient catalysts in some of the important heterogeneous reactions such as the generation of carbon nanotubes by catalytic cracking of methane,[5] synthesis of vertically aligned carbon nanofibers,[6] methane decomposition,[7] high-temperature water-gas shift reaction,[8] synthesis of higher alcohols from syngas,[9] the hydrogenation of *p*-chloronitrobenzene,[10] and selective oxidation of ethyl benzene.[11]

Over the past decade, inorganic material–nanoparticles have gained increasing attention in the pharmaceutical industry due to their strong antibacterial properties and biocompatibility.[12] For example, Ag–Cu and Ni–Ag, Cu–Ni, Ag–Au, and Ni–Co NPs exhibit antibacterial properties,[13,14] with widespread applications in dental and hyperthermia,[15,16] the biological activities toward human mesenchymal stem cells (hMSC),[17] and non-enzymatic glucose sensor applications,[18] respectively.

Heterocyclic systems are common structural motifs in many biologically active compounds and therefore intense effort has been devoted by researchers constantly to introduce newer and efficient protocols for their synthesis. Coumarin and its derivatives are a large group of heterocycles with a wide variety of biological and therapeutic properties such as anti-HIV,[19] cytotoxicity and enzyme inhibitory,[20] anti-fungal,[21] anti-bacterial,[22] anti-oxidant,[23] anti-cancer,[24] and anti-coagulant properties.[25] Among coumarin derivatives, biscoumarins become more popular and are usually prepared by the condensation reaction of aldehydes with 4-hydroxycoumarin. This reaction can be catalyzed by several types of catalysts such as piperidine,[26] I_2,[27] sodium dodecyl sulfate,[28] [poly(4-vinylpyridine) $BuSO_3H$]Cl.x$AlCl_3$,[29] MW irradiation,[30,31] [poly(4-vinylpyridine)–$BuSO_3H$]HSO_4,[32] indion 190 resin,[33] choline hydroxide,[34] poly(AMPS-*co*-AA)@Fe_3O_4,[35] $Zn(OAc)_2$,[36] and triethylammonium hydrogen sulfate.[37] However, these methods are plagued by the limitation of prolonged reaction times, low yields, tedious work up, inefficiency of method when aliphatic aldehydes are used in the reaction, and the use of expensive, hazardous, difficult to handle or unreusable catalysts.

Various synthetic techniques have been reported for preparing nanoalloys such as reduction method, interaction

CONTACT Kaveh Parvanak Boroujeni parvanak-ka@sci.sku.ac.ir Department of Chemistry, Shahrekord University, Shahrekord, (115), Iran.
Color versions of one or more of the figures in the article can be found online at www.tandfonline.com/lsrt.

method, vapor quenching, sputtering and gas condensation.[38,39] Among them, the reduction method is relatively the simplest one. During the reduction process, if the two metals in a complex have different redox potential, they will form a core-shell structure, otherwise they generate bimetallic alloy.[40,41] Along this line and in continuation of our works on the synthesis and applications of magnetic catalysts, nanoalloys, and heterogeneous catalysts[35,39,42,43] we now wish to introduce bimetallic and trimetallic magnetic nanoalloys base on cupper as new magnetic catalysts for the synthesis of biscoumarins. Also, anti-bacterial, anti-oxidant, and DNA cleavage properties of these NPs were investigated.

Experimental

Materials and methods

All chemicals were either prepared in our laboratory or were purchased from Merck and Fluka. Two bacterial strains were used: *E. coli* (ATCC 35218) and *S. aureus* (ATCC 6538). Reaction monitoring and purity determination of the products were accomplished by GLC or TLC on silica-gel polygram SILG/UV254 plates. Gas chromatography was recorded on Shimadzu GC 14–A. IR spectra were obtained by a Shimadzu model 8300 FT–IR spectrophotometer. ^{1}H NMR spectra were recorded on 400 MHz spectrometer in $CDCl_3$. Melting points were determined on a Fisher–Jones melting–point apparatus. XRD patterns were recorded by a Phillips, X–ray diffractometer using graphite monochromatized Cu Kα radiation. A morphological study of the synthesized products was carried out directly by a Hitachi S4160 field emission scanning electron microscope (FE–SEM). Room temperature magnetic properties were investigated by Lakeshore device in an applied magnetic field sweeping between ±8000 Oe.

Preparation of Cu–Ni NPs[39]

0.1 g of $[Cu(NH_3)_4][Ni(C_2O_4)_2]$ complex (0.27 mmol) was dissolved in 20 mL of a mixture of water-ethanol solution (50:50). Then, to stirred solution, 5 mL of hydrazine and 10 mL of NaOH (4 M) were gradually added at 70–80 °C. During the reduction reaction the color of the solution was turned to red and then after 1 h the black Cu–Ni NPs were observed. The resulting black NPs were carefully decanted, washed repeatedly with doubly distilled water, and dried at room temperature for 24 h.

Preparation of Cu–Ni–Ag NPs

In the preparation of the above Cu-Ni nanoalloy after addition of hydrazine and NaOH solution at 70–80 °C, a solution of silver nitrate (0.1 M, 2.7 mL) and then hydrazine (2 mL) were gradually added to the reaction solution to yield Cu–Ni–Ag NPs.

Preparation of 3,3′-(4-bromobenzylidene)-bis-(4-hydroxycoumarin) as a typical procedure for the synthesis of biscoumarins

To a solution of 4-bromobenzaldehyde (1 mmol), 4-hydroxycoumarin (2 mmol), and toluene (3 mL), Cu–Ni (0.05 g) or Cu–Ni–Ag (0.04 g) was added at 90 °C. After the completion of the reaction (monitored by TLC), the catalyst was removed by an external magnet and washed with toluene (2 × 5 mL) and the filtrate was concentrated on a rotary evaporator under reduced pressure. Whenever required, the crude product was recrystallized from ethanol to give the pure product.

Antibacterial test performance

At first, *E.coli* and *S.aureus* cells were separately transferred from pure bacterial stocks to nutrient broth media, and incubated at 37 °C until reaching to 0.5 McFarland standard. The diffusion method is provided by the application of standard bacterial inoculums to the surface of Muller-Hinton agar plates (100 mm diameter) using sterile swabs. After incubation of plates at 37 °C for 24 h and bacterial growth, distinct equal wells have been created in the agar plates for antibacterial diffusion assay. Then, dispersed solutions of Cu–Ni and Cu–Ni–Ag NPs were individually poured into the wells with distinct concentrations (0.25, 0.5, 1 or 2 mg/mL). After incubation at 37 °C for 18–24 hours, the growth inhibition zone diameters (in millimeter scale) was determined. Standard antibiotic discs and sterile distilled water has been used as positive and negative controls, respectively.

DPPH radical–scavenging activity

The 0.1 mM DPPH in methanol solution was prepared. 450 µL of Tris–HCl buffer (pH= 7.4) and 1 mL of methanolic DPPH solution were added to 50 µL of Cu–Ni and Cu–Ni–Ag NPs with distinct concentrations (2.5, 5, 10 or 20 µg/mL). The mixtures were left for 30 min at room temperature in the dark and then their absorbance was measured at 517 nm. The methanol was applied as a blank solution. The same experiment was performed with BHT as a positive control. The DPPH free radical scavenging activity was calculated by the following equation: %DPPH radical scavenging = $Absorbance_{(blank)} - Absorbance_{(sample)}/Absorbance_{(blank)} \times 100$.

DNA cleavage assays

The cleavage of pET-28 plasmid DNA by Cu–Ni and Cu–Ni–Ag NPs was identified using agarose gel electrophoresis. Each 40 µL of Cu–Ni and Cu–Ni–Ag NPs with distinct concentrations (0.25, 0.5, 1 or 2 mg/mL) was mixed with 5 µL of plasmid DNA solution (0.25 µg/mL) in sterile 1.5 mL micro tubes and incubated at 37 °C for 24 h. Then 10 µL of the resulting mixture was mixed with 1 µL of gel loading dye (G2526-5ML Sigma-Aldrich) and loaded into the 1% agarose gel (W/V) wells. The agarose gel was prepared with

TBE 1X buffer (Tris-HCl (0.07 M, pH= 7.4), EDTA (4 mL, 0.5 M, pH= 8.0), and boric acid (5.5 g)) in distilled water (1 L). After performing electrophoresis (40 mA and 80 volt for 45 min), the final agarose gel was observed in the gel duct device (UVItec Limited BTS-20M) under UV rays.

Results and discussion

Synthesis and characterization of Cu–Ni and Cu–Ni–Ag NPs

In our previous work, the bimetallic nanoalloys Cu–Ni was produced from the by chemical reduction of the $[Cu(NH_3)_4][Ni(C_2O_4)_2]$ using hydrazine.[39] In this work the reduction of this complex along with silver nitrate ($AgNO_3$) by excess hydrazine lead to formation of Cu–Ni–Ag NPs. During the reduction process, the whole reaction proceeds through co-reduction of Cu^{2+}, Ni^{2+} and Ag^{+} so solid solution Cu–Ni–Ag NPs is formed. The reactions can take place at 70–80 °C in water-ethanol solution via the following equations.

$$[Cu(NH_3)_4][Ni(C_2O_4)_2] + N_2H_4 + 4NaOH \rightarrow \mathbf{Cu\text{–}Ni} + N_2 + 4NH_3 + 2Na_2C_2O_4 + 4H_2O$$

$$[Cu(NH_3)_4][Ni(C_2O_4)_2] + AgNO_3 + 5/4N_2H_4 + 5NaOH \rightarrow \mathbf{Cu\text{–}Ni\text{–}Ag} + 5/4N_2 + 4NH_3 + 2Na_2C_2O_4 + NaNO_3 + 5H_2O$$

The crystal structure of these Cu–Ni bimetallic and Cu–Ni–Ag trimetallic NPs was studied by powder X–ray diffraction (XRD). The powder diffraction pattern of Cu–Ni bimetallic have been studied completely (Figure 1a).[39] The diffraction peaks for Cu–Ni–Ag NPs shows that this nanoalloy is in the face-center cubic (fcc) phase and also confirm that these compounds can be considered as Cu/Ni/Ag trimetallic NPs. In Figure 1b three distinct diffraction peaks are clearly observed at 2θ values of 43.50, 50.64 and 74.32° that could be assigned to 111, 200 and 220 crystal planes of the metallic Cu, respectively. The results show that diffraction peaks are in good agreement with the standard values for Cu (with card no. 04-0836), nickel (with card no. 87-0712) and silver (with card no. 01-1164). In most studies of the grain size of nanocrystalline materials, X–ray line-broadening analysis is used. The crystallite size is estimated from the full width at half maximum (FWHM) of the diffraction peaks by the Scherrer formula. The crystal siza obtained for Cu–Ni and Cu–Ni–Ag NPs, relationship at the sharpest peak are 29 and 44 nm, respectively.

FT–IR of Cu–Ni[39] and Cu–Ni–Ag NPs are shown in Figure 2. In the conversion of complex into NPs, the absorption bands related to the ligand groups in complex were disappeared and the metals had no absorption bands in the medium IR region. However, the weak absorption bands due to the water in the alloy NPs are observed in the infrared spectrum.

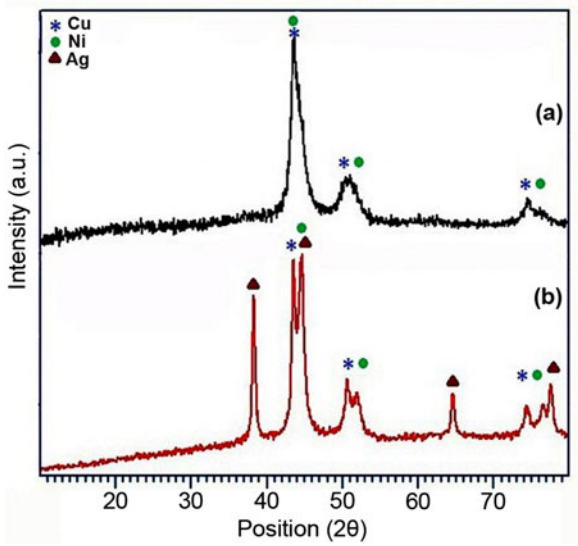

Figure 1. X-Ray diffraction patterns for (a) Cu–Ni and (b) Cu–Ni–Ag NPs.

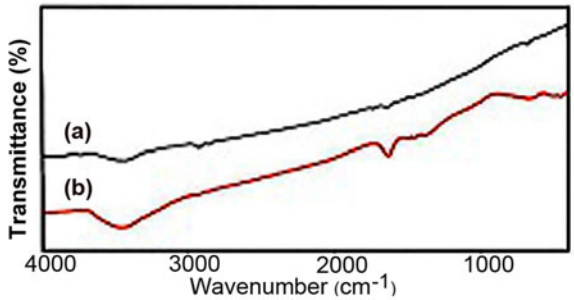

Figure 2. FT–IR spectra of (a) Cu–Ni and (b) Cu–Ni–Ag NPs.

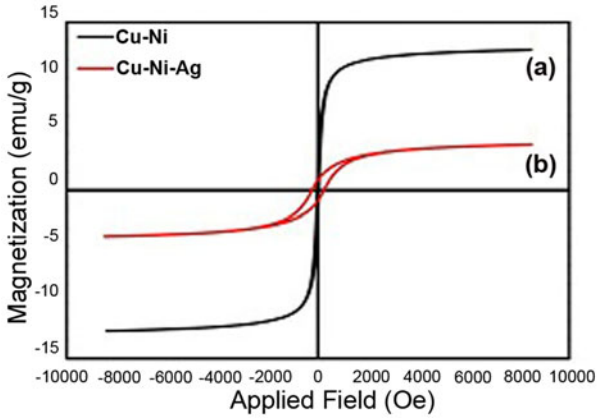

Figure 3. The magnetization curves and saturation magnetizations of (a) Cu–Ni[39] and (b) Cu–Ni–Ag NPs.

Magnetic properties of bimetallic and trimetallic NPs were also studied. As show in Figure 3, NPs are characteristic of ferromagnetic material. The saturation magnetization (Ms) values of Cu–Ni and Cu–Ni–Ag NPs are 13 and 5 emu/g, at 300 K, respectively, that confirm trimetallic alloy NPs have Ms less than the bimetallic alloy and the nickel NPs have a Ms less than that of the bulk nickel (about 55 emu/g at 300 K[44]). Also, the magnetic properties of NPs show that the Ms decreases with increasing Cu and Ag concentration. The reason of the decrease in Ms of Cu–Ni and

Cu–Ni–Ag NPs is due to the presence of dissolved Ni in the Cu and Ag matrix (Figure 3b).

The FE–SEM studies from Figure 4a show monodisperse, spherical and uniform particles of Cu–Ni by average diameter size 15 nm.[39] The images of SEM revealed that uniform particles morphology in Cu–Ni changed by increasing the presence of silver, therefore images of Cu–Ni–Ag samples (Figure 4b) show agglomeration of particles with different size in spherical shapes. The particle size distribution graphs for Cu–Ni–Ag samples obtained from FE–SEM analysis, according to which the average diameter of maximum number of particles lies in the range of 30–40 nm.

The different dispersion of the formed nanoalloy phases can be also argued by considering energy-dispersive X–ray (EDX) data in SEM micrographs. EDX analysis shows that these prepared NPs are pure nanoalloys (Figure 5).

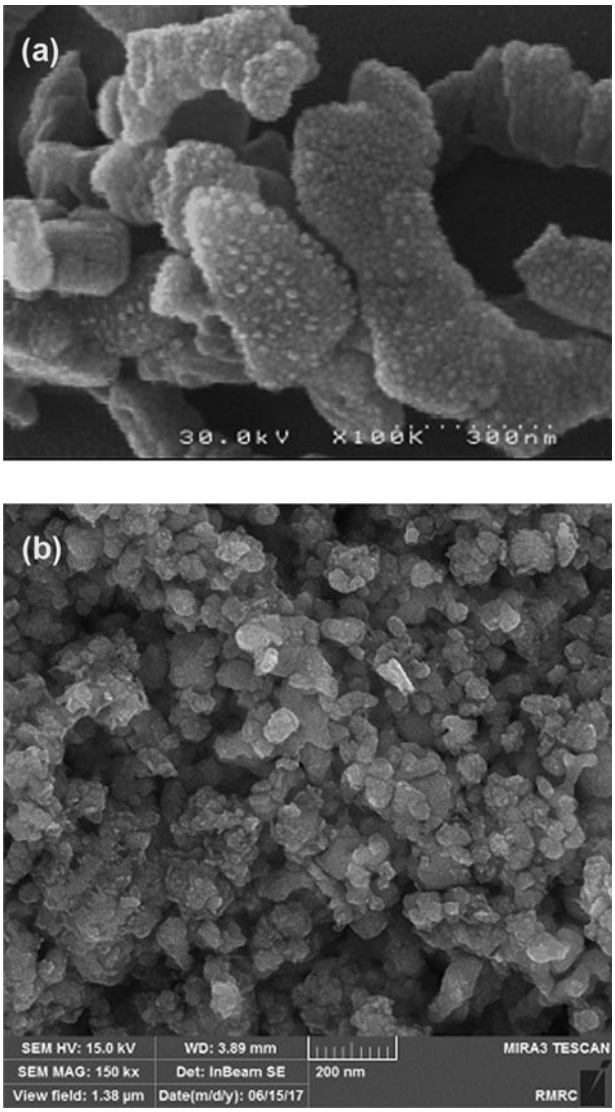

Figure 4. SEM images of (a) Cu–Ni and (b) Cu–Ni–Ag NPs.

Catalytic application of Cu–Ni and Cu–Ni–Ag NPs in the synthesis of biscoumarins

The catalytic performance of NPs was investigated in the condensation reaction of aldehydes with 4-hydroxycoumarin. For this purpose, as a model reaction, reaction of 4-bromobenzaldehyde (1 mmol) with 4-hydroxycoumarin (2 mmol) in the presence of different amounts of NPs in various solvents and also under solvent free conditions were studied. We observed that this reaction was performed smoothly in toluene at 90 °C in the presence of 0.05 g of Cu–Ni or 0.04 g of Cu–Ni–Ag NPs and the desired product 3,3'-(4-bromobenzylidene)-bis-(4-hydroxycoumarin) was obtained in excellent yield (Table 1, entry 4). Afterwards, under the optimized conditions, various aromatic (entries 1–10), heteroaromatic (entries 11,12), and aliphatic aldehydes (entries 13–15) were reacted with 4-hydroxycoumarin and the corresponding products were obtained in excellent yields. As the results in Table 1 show, the better yields were obtained with aromatic aldehyde containing electron withdrawing groups (entries 9,10). This can be explained by the reaction mechanism in Scheme 1. Aldehyde forms an oxygen-bonded complex through NPs to give activated aldehyde, which is attacked by of 4-hydroxycoumarin to afford the intermediate I. Then, the intermediate II is produced by dehydration of the intermediate I. The 1,4-nucleophilic addition of a second molecule of 4-hydroxycoumarin on activated intermediate II, in the Michael addition fashion, affords the synthesis of biscoumarin product. The electron withdrawing groups substituted on aromatic aldehyde in intermediate II increase the rate of 1,4-nucleophilic addition reaction because of the alkene LUMO is at lower energy in their presence compared with electron donating groups.[29]

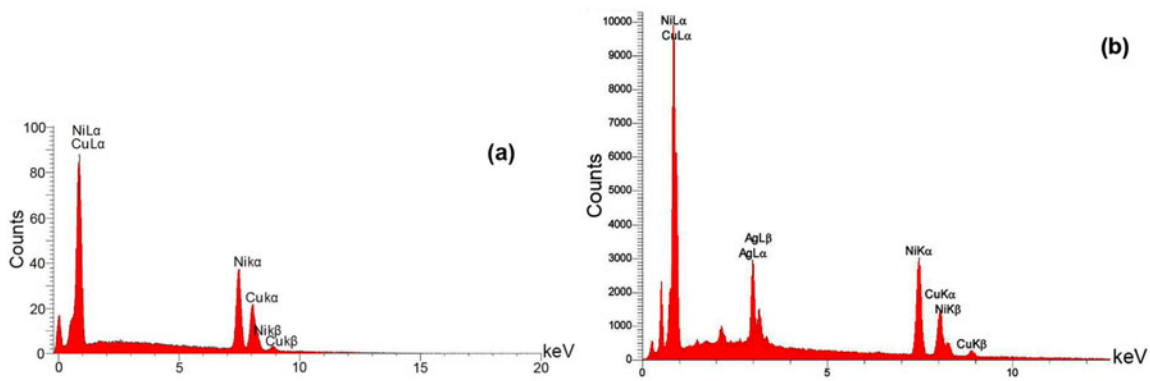

Figure 5. EDX spectrum of (a) Cu–Ni[39] and (b) Cu–Ni–Ag NPs.

Table 1. Synthesis of biscoumarin derivatives catalyzed by Cu–Ni and Cu–Ni–Ag NPs.

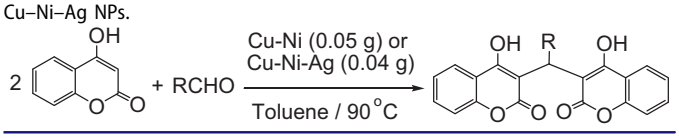

Entry	Aldehyde	Time (min.)	Yield (%)[a,b]	M.P. (°C)	
				Found	Lit.
1	C_6H_5	20^1,15^2	97^1,98^2	229–231	226–228[31]
2	4-$CH_3C_6H_4$	22^1,16^2	95^1,96^2	260–262	265–266[30]
3	4-$CH_3OC_6H_4$	25^1,20^2	96^1,97^2	242–244	244–246[31]
4	4-BrC_6H_4	20^1,17^2	97^1,98^2	264–266	268–270[30]
5	4-ClC_6H_4	20^1,16^2	94^1,95^2	256–257	254–256[31]
6	3-ClC_6H_4	20^1,16^2	94^1,95^2	220–222	215[26]
7	4-HOC_6H_4	23^1,20^2	95^1,96^2	227–229	220–224[30]
8	3-HOC_6H_4	25^1,20^2	95^1,96^2	213-214	210.5[26]
9	4-$NO_2C_6H_4$	15^1,10^2	97^1,98^2	233–234	236–237[31]
10	3-$NO_2C_6H_4$	16^1,10^2	96^1,97^2	238–240	233–234[30]
11	2-Thienyl	20^1,18^2	93^1,95^2	214–216	213-214[30]
12	2-Furanyl	20^1,17^2	94^1,96^2	201–203	204-205[30]
13	$C_6H_5CH=CH$	29^1,24^2	94^1,94^2	200-202	196[26]
14	$C_6H_5CH_2CH_2$	25^1,22^2	93^1,92^2	189–191	190-193[32]
15	$CH_3(CH_2)_2$-	30^1,23^2	94^1,93^2	125–126	123[26]

[a]Isolated yields.
[b]All products are known compounds and were identified by comparison of their physical and spectral data with those of the authentic samples.

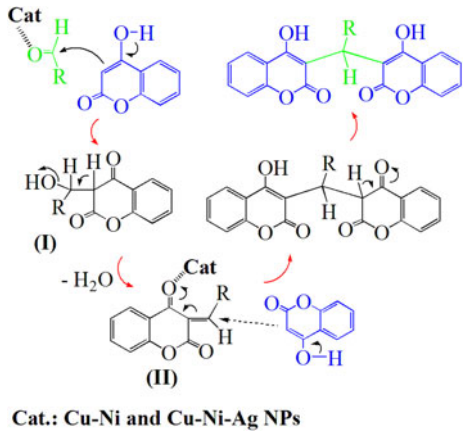

Scheme 1. Suggested mechanism for the preparation of biscoumarins catalyzed by Cu–Ni and Cu–Ni–Ag NPs.

^{1}H NMR spectra of the 3,3'-(4-bromobenzylidene)-bis-(4-hydroxycoumarin) is shown in Figure 6.

Recently, we have reported carbon nanotube-supported butyl 1-sulfonic acid groups and cellulose aluminum oxide composite-supported imidazolium chloroaluminate ionic liquid as heterogeneous catalysts for the synthesis of xanthene deravatives.[42,43] Along this line and based on the above results, we found that Cu–Ni and Cu–Ni–Ag NPs can be used as magnetic catalysts for the synthesis of 1,8-dioxo-octahydroxanthenes through condensation of aromatic aldehydes with two equivalents of dimedone in ethanol at room temperature (Scheme 2).

The stability and reusability of a catalyst are very important factors for industrial use. Thus, the recovery and reusability of Cu–Ni and Cu–Ni–Ag NPs were investigated and it was found that the catalysts could be completely recovered and used again at least six times without any noticeable loss of catalytic activity (Figure 7).

Finally, we present a comparison between selected previously known catalysts and Cu–Ni and Cu–Ni–Ag NPs employed for the synthesis of biscoumarins. As shown in Table 2, in comparison with many of catalysts Cu–Ni and Cu–Ni–Ag NPs have good catalytic performance in terms of high yields at short reaction times, reusability, easy separation, and mild reaction conditions.

The investigation of biological activity of Cu–Ni and Cu–Ni–Ag NPs

The main objective of antibacterial tests is the evaluation of the resistance of bacteria to chosen empirical antimicrobial agents.[45] For this purpose, one of the simplest tests includes the manual method which itself is classified in two different methods containing disk and gradient diffusion. The first one has several advantages such as its simplicity, requirement of simple equipment, flexibility in choice of disks, and relatively lower costs.[45]

Encouraged by the results obtained from the catalytic activity of Cu–Ni and Cu–Ni–Ag NPs in the synthesis of biscoumarins and xanthenes derivatives, we also investigated the anti-bacterial properties of these NPs on viable typical microorganisms. Antibacterial activity of NPs was studied against gram positive and gram negative bacteria using disk diffusion method and the zone of growth inhibition was measured quantitatively (Figure 8a–d, Table 3). As the results show, Cu–Ni–Ag NPs have stronger degree of antibacterial activity than Cu–Ni NPs. Cu–Ni and Cu–Ni–Ag NPs both exhibit antibacterial properties against *E.coli* cell. Cu–Ni NPs do not show antibacterial activity against *S.aureus* cell, while Cu–Ni–Ag NPs have an efficient antibacterial effect on it, which can be attributed to the presence of Ag in this triple alloy and its antibacterial features.[13] The growth inhibition zone of two bacteria increased with increment of the concentration of NPs.

Oxidation is a chemical reaction that can produce free radicals, leading to chain reactions that may promote some of illnesses such as cancer. Antioxidants agents are able to terminate these chain reactions and hence limit harmful effects of cellular oxidants. Reactive oxygen species (ROS) and reactive nitrogen species (RNS) are two types of cellular oxidants which are produced in living cells.[46] Recently, nanotechnology is focusing on synthesis of NPs having improved antioxidant properties which can be used for prevention or treatment of diseases. A convenient method for the determination of antioxidant activity of NPs is radical scavenging method which in 2,2-diphenyl-2-picrylhydracyl hydrate (DPPH) is used as a stable compound which accepts electrons from antioxidant donors.[47]

Following the obtained results of antibacterial tests, we tried to evaluate antioxidant activity of these NPs with distinct concentrations (2.5, 5, 10, and 20 µg/mL) using DPPH. As shown in Figure 9, effective free radical inhibition was observed for Cu–Ni and Cu–Ni–Ag NPs. The antioxidant activity of the Cu–Ni NPs were lower than butyl hydroxytoluene (BHT) and the antioxidant activity of the Cu–Ni–Ag

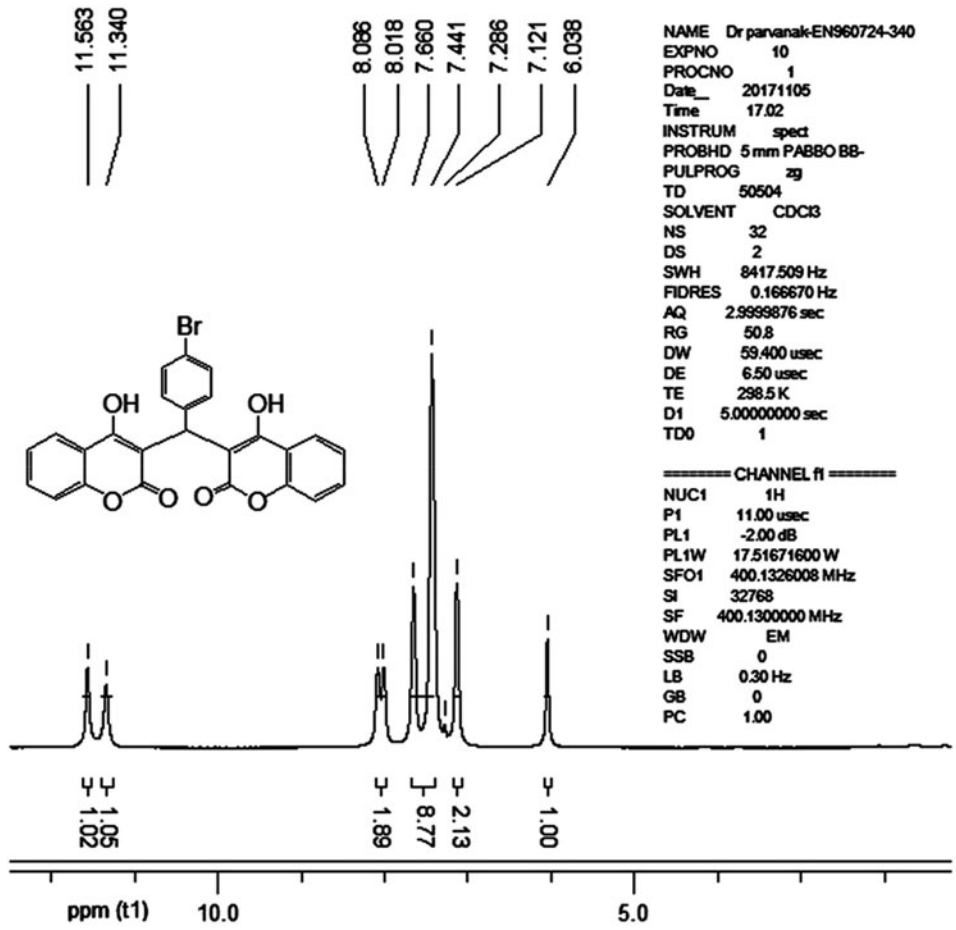

Figure 6. [1]H NMR spectra of the 3,3′-(4-bromobenzylidene)-bis-(4-hydroxycoumarin).

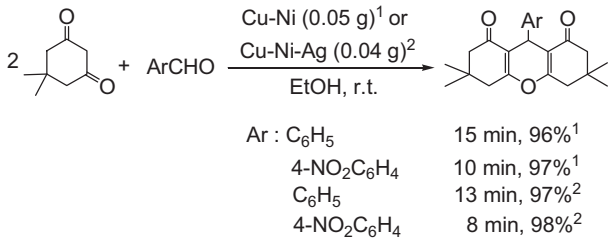

Scheme 2. Preparation of 1,8-dioxo-octahydroxanthenes using Cu–Ni and Cu–Ni–Ag NPs.

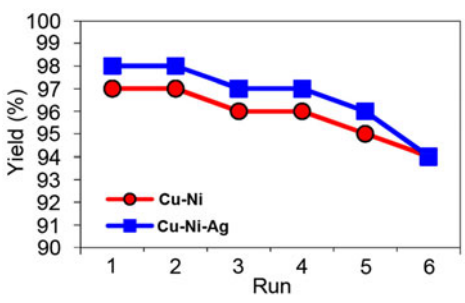

Figure 7. Recyclability of Cu–Ni (0.05 g) and Cu–Ni–Ag (0.04 g) NPs in the reaction of 4-nitrobenzaldehyde (1 mmol) with 4-hydroxycoumarin (2 mmol) in toluene at 90 °C after 15 and 10 min, respectively.

Table 2. Comparison of the catalytic efficiency of Cu–Ni and Cu–Ni–Ag NPs with selected previously catalysts in the condensation reaction of benzaldehyde with two equivalents of 4-hydroxycoumarin.

Entry	Reaction conditions	Time (min.)	Yield (%)a
1	Piperidine, EtOH, r.t.	240	92[26]
2	I_2, H_2O, 100 °C	25	97[27]
3	Sodium dodecyl sulfate, H_2O, 60 °C	138	90[28]
4	[Poly(4-vinylpyridine)-$BuSO_3H$]Cl-x$AlCl_3$, toluene, 90 °C	36	95[29]
5	Catalyst-free, solvent-free, MW Irradiation, r.t.	3.5	91[30]
6	Catalyst-free, H_2O, MW irradiation, r.t.	48	93[31]
7	[Poly(4-vinylpyridine)-$BuSO_3H$]HSO_4, toluene, 90 °C	5	98[32]
8	Indion 190 resin, toluene, 100 °C	30	90[33]
9	Aaqueous solution of choline hydroxide, 50 °C	60	99[34]
10	Poly(AMPS-*co*-AA)@Fe_3O_4, toluene, 90 °C	15	97[35]
11	$Zn(OAc)_2$, H_2O, 100 °C	25	98[36]
12	Triethylammonium hydrogen sulfate, EtOH, 80 °C	30	88[37]
13	Cu-Ni NPs, toluene, 90 °C	20	97
14	Cu-Ni-Ag NPs, toluene, 90 °C	15	98

[a]Isolated yields.

NPs was higher than Cu–Ni NPs. The IC50 value of the Cu–Ni and Cu–Ni–Ag NPs has been shown in Table 4.

The damage of genomic DNA can be caused by oxygen and nitrogen free radicals.[48] It can lead to chromosomal abnormalities such as chromatin fractures that promote cell death or uncontrolled cell proliferation. Thus, studies on the

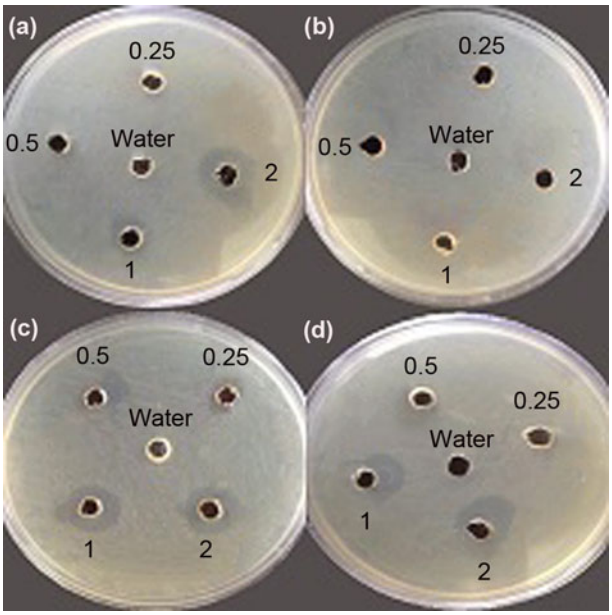

Figure 8. Evaluation of the antimicrobial activity of a) Cu–Ni NPs against *E.coli*; b) Cu–Ni NPs against *S.aureus*; c) Cu–Ni–Ag NPs against *E.coli*; d) Cu–Ni–Ag NPs against *S.aureus*.

Table 3 Antibacterial activity of Cu–Ni and Cu–Ni–Ag NPs

	Zone of growth inhibition[a] (mm)/ Concentration (mg/mL)				Zone of growth inhibition[b] (mm)/ Concentration (mg/mL)			
Species	0.25	0.5	1	2	0.25	0.5	1	2
E.coli	1	1	5	8	2	6	7	8
S.aureus	–	–	–	–	–	1	8	11

[a]Cu–Ni NPs.
[b]Cu–Ni–Ag NPs.

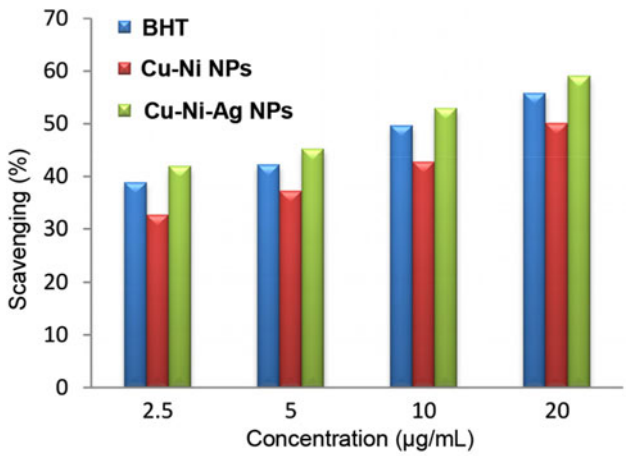

Figure 9. The DPPH radical scavenging activity of the BHT, Cu–Ni, and Cu–Ni–Ag NPs.

DNA cleavage by synthetic materials such as NPs have been the subject of great interest to researchers.[47]

After evaluation of antibacterial and antioxidant activities of the Cu–Ni and Cu–Ni–Ag NPs, we also examined DNA cleavage property of these NPs. The cleavage of plasmid DNA was revealed by gel electrophoresis. In agarose gel electrophoresis method DNA molecules migrate in the gel texture based on their charge, size, and topology. Figure 10.

Table 4. The IC_{50} values of the BHT, Cu–Ni, and Cu–Ni–Ag NPs.

Sample	IC_{50} (µg/mL)
BHT	12.53 ± 2.43
Cu–Ni NPs	19.12 ± 2.89
Cu–Ni–Ag NPs	9.62 ± 2.09

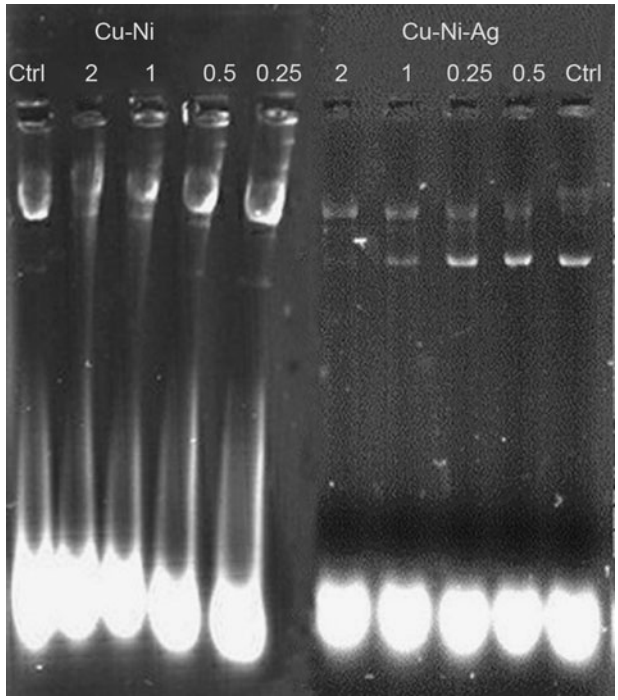

Figure 10. Effect of the distinct concentrations of Cu–Ni and Cu–Ni–Ag NPs (0.25, 0.5, 1, and 2 mg/mL) on the DNA cleavage.

shows gel electrophoretic pattern of DNA after incubation with distinct concentrations of Cu–Ni and Cu–Ni–Ag NPs in contrast to plasmid DNA mixed with water as the negative control. After exposure of plasmid DNA to different concentrations of the nanomaterial suspensions no destructive effects were observed on DNA.

Conclusion

In conclusion, we prepared Cu–Ni and Cu–Ni–Ag NPs and investigated their application as magnetic catalysts for the synthesis of biscoumarin and xanthene derivatives. The catalysts were easily separated from the reaction media by the application of an external magnetic and work-up of these reactions is very easy. The products were obtained in high yields in short reaction times and the recycled catalysts can be used for further reactions without any activity loss. Biological activity of these NPs such as anti-bacterial, anti-oxidant, and DNA cleavage properties were also investigated. The results showed that both Cu–Ni and Cu–Ni–Ag NPs have antibacterial and antioxidant properties and they had no significant effect on DNA cleavage.

Acknowledgements

The author thanks the Research Council of Shahrekord University for partial support of this work.

References

[1] Habashi, F. *Alloys: Preparation, Properties, Applications*, New York: Wiley, **2008**.

[2] Dorantes-Dávila, J.; Pastor, G. M. Nanoalloys; Calvo, F. Eds.; Elsevier Inc: Paris, **2013**, 247–274.

[3] Roozmeh, S.; Mohseni, S.; Tehranchi, M. Study of Magnetoimpedance Effect of Co-based Amorphous Ribbons after Current Annealing at Various Kinds of Ambient Pressure. *J. Non-Cryst. Solids* **2009**, *355*, 2653–2656. DOI: 10.1016/j.jnoncrysol.2009.09.002.

[4] Chaturvedi, S.; Dave, P. N.; Shah, N. K. Applications of Nano-catalyst in New Era. *J. Saudi Chem. Soc* **2012**, *16*, 307–325. DOI: 10.1016/j.jscs.2011.01.015.

[5] González, I.; De Jesus, J. C.; de Navarro, C. U.; García, M. Effect of Cu on Ni Nanoparticles Used for the Generation of Carbon Nanotubes by Catalytic Cracking of Methane. *Catal. Today* **2010**, *149*, 352–357. DOI: 10.1016/j.cattod.2009.07.101.

[6] Klein, K. L.; Melechko, A. V.; Rack, P. D.; Fowlkes, J. D.; Meyer, H. M.; Simpson, M. L. Cu–Ni Composition Gradient for the Catalytic Synthesis of Vertically Aligned Carbon Nanofibers. *Carbon* **2005**, *43*, 1857–1863. DOI: 10.1016/j.carbon.2005.02.027.

[7] Wang, H. Y.; Lua, A. C. Methane Decomposition Using Ni–Cu Alloy Nano-particle Catalysts and Catalyst Deactivation Studies. *Chem. Eng. J.* **2015**, *262*, 1077–1089. DOI: 10.1016/j.cej.2014.10.063.

[8] Saw, E. T.; Oemar, U.; Tan, X. R.; Du, Y.; Borgna, A.; Hidajat, K.; Kawi, S. Bimetallic Ni–Cu Catalyst Supported on CeO_2 for High-temperature Water–Gas Shift Reaction: Methane Suppression via Enhanced CO Adsorption. *J. Catal.* **2014**, *314*, 32–46. DOI: 10.1016/j.jcat.2014.03.015.

[9] Liu, G. L.; Niu, T.; Cao, A.; Geng, Y. X.; Zhang, Y.; Liu, Y. The Deactivation of Cu–Co Alloy Nanoparticles Supported on ZrO2 for Higher Alcohols Synthesis from Syngas. *Fuel* **2016**, *176*, 1–10. DOI: 10.1016/j.fuel.2016.02.057.

[10] Han, X.; Zhou, R.; Lai, G.; Zheng, X. Influence of Support and Transition Metal (Cr, Mn, Fe, Co, Ni and Cu) on the Hydrogenation of *p*-chloronitrobenzene over Supported Platinum Catalysts. *Catal. Today* **2004**, *93*, 433–437. DOI: 10.1016/j.cattod.2004.06.053.

[11] Xie, R.; Fan, G.; Yang, L.; Li, F. Hierarchical Flower-like Co–Cu Mixed Metal Oxide Microspheres as Highly Efficient Catalysts for Selective Oxidation of Ethylbenzene. *Chem. Eng. J.* **2016**, *288*, 169–178. DOI: 10.1016/j.cej.2015.12.004.

[12] Guo, J.; Wang, X.; Miao, P.; Liao, X.; Zhang, W.; Shi, B. One-step Seeding Growth of Controllable Ag@Ni Core–shell Nanoparticles on Skin Collagen Fiber with Introduction of Plant Tannin and Their Application in High-performance Microwave Absorption. *J. Mater. Chem.* **2012**, *22*, 11933–11942. DOI: 10.1039/c2jm30370a.

[13] Taner, M.; Sayar, N.; Yulug, I. G.; Suzer, S. Synthesis, Characterization and Antibacterial Investigation of Silver–Copper Nanoalloys. *J. Mater. Chem.* **2011**, *21*, 13150–13154. DOI: 10.1039/c1jm11718a.

[14] Senapati, S.; Srivastava, S. K.; Singh, S. B.; Mishra, H. N. Magnetic Ni/Ag Core–shell Nanostructure from Prickly Ni Nanowire Precursor and Its Catalytic and Antibacterial Activity. *J. Mater. Chem.* **2012**, *22*, 6899–6906. DOI: 10.1039/c2jm00143h.

[15] Argueta-Figueroa, L.; Morales-Luckie, R. A.; Scougall-Vilchis, R. J.; Olea-Mejía, O. F. Synthesis, characterization and Antibacterial Activity of Copper, nickel and Bimetallic Cu–Ni Nanoparticles for Potential Use in Dental Materials. *Prog. Nat. Sci.* **2014**, *24*, 321–328. DOI: 10.1016/j.pnsc.2014.07.002.

[16] Chatterjee, J.; Bettge, M.; Haik, Y.; Chen, C. J. Synthesis and Characterization of Polymer Encapsulated Cu–Ni Magnetic Nanoparticles for Hyperthermia Applications. *J. Magn. Mater* **2005**, *293*, 303–309. DOI: 10.1016/j.jmmm.2005.02.024.

[17] Mahl, D.; Diendorf, J.; Ristig, S.; Greulich, C.; Li, Z. A.; Farle, M.; Köller, M.; Epple, M. Silver, gold, and Alloyed Silver–Gold Nanoparticles: Characterization and Comparative Cell-biologic Action. *J. Nanopart. Res.* **2012**, *14*, 1153–1155.

[18] Ranjani, M.; Sathishkumar, Y.; Lee, Y. S.; Jin Yoo, D.; Kim, A. R.; Gnana Kumar, G. Ni–Co Alloy Nanostructures Anchored on Mesoporous Silica Nanoparticles for Non-enzymatic Glucose Sensor Applications. *RSC Adv.* **2015**, *5*, 57804–57814. DOI: 10.1039/C5RA08471G.

[19] Su, C. X.; Mouscadet, J. F.; Chiang, C. C.; Tsai, H. J.; Hsu, L. Y. HIV-1 Integrase Inhibition of Biscoumarin Analogues. *Chem. Pharm. Bull.* **2006**, *54*, 682–686.

[20] Kostova, I.; Momekov, G.; Zaharieva, M.; Karaivanova, M. Cytotoxic Activity of New Lanthanum (III) Complexes of Bis-Coumarins. *Eur. J. Med. Chem* **2005**, *40*, 542–551. DOI: 10.1016/j.ejmech.2004.12.007.

[21] Brooker, N. L.; Kuzimichev, Y.; Laas, J.; Pavlis, R. Evaluation of Coumarin Derivatives as Anti-fungal Agents against Soil-borne Fungal Pathogens. *Commun. Agric. Appl. Biol. Sci.* **2007**, *72*, 785–793.

[22] Kong, Y.; Fu, Y. J.; Zu, Y. G.; Chang, F. R.; Chen, Y. H.; Liu, X. L.; Stelten, J.; Schiebel, H. M. Cajanuslactone, a New Coumarin with Anti-bacterial Activity from Pigeon Pea [*Cajanus cajan* (L.) Millsp.] Leaves. *Food Chem* **2010**, *121*, 1150–1155. DOI: 10.1016/j.foodchem.2010.01.062.

[23] Hamdi, N.; Puerta, M. C.; Valerga, P. Synthesis, Structure, Antimicrobial and Antioxidant Investigations of Dicoumarol and Related Compounds. *Eur. J. Med. Chem.* **2008**, *43*, 2541–2548. DOI: 10.1016/j.ejmech.2008.03.038.

[24] Carta, F.; Maresca, A.; Scozzafava, A.; Supuran, C. T. Novel Coumarins and 2-thioxo-coumarins as Inhibitors of the Tumor-associated Carbonic Anhydrases IX and XII. *Bioorg. Med. Chem.* **2012**, *20*, 2266–2273. DOI: 10.1016/j.bmc.2012.02.014.

[25] Monti, M.; Pinotti, M.; Appendino, G.; Dallocchio, F.; Bellini, T.; Antognoni, F.; Poli, F.; Bernardi, F. Characterization of Anti-coagulant Properties of Prenylated Coumarin Ferulenol. *Biochim. Biophys. Acta* **2007**, *1770*, 1437–1440. DOI: 10.1016/j.bbagen.2007.06.013.

[26] Khan, K. M.; Iqbal, S.; Lodhi, M. A.; Maharvi, G. M.; Ullah, Z.; Choudhary, M. I.; Rahman, A.-U.; Perveen, S. Biscoumarin: New Class of Urease Inhibitors; Economical Synthesis and Activity. *Bioorg. Med. Chem.* **2004**, *12*, 1963–1968. DOI: 10.1016/j.bmc.2004.01.010.

[27] Kidwai, M.; Bansal, V.; Mothsra, P.; Saxena, S.; Somvanshi, R. K.; Dey, S.; Singh, T. P. Molecular Iodine: A Versatile Catalyst for the Synthesis of Bis (4-hydroxycoumarin) Methanes in Water. J. Mol. Catal. A. *Chem.* **2007**, *268*, 76–81. DOI: 10.1016/j.molcata.2006.11.054.

[28] Mehrabi, H.; Abusaidi, H. Synthesis of Biscoumarin and 3, 4-dihydropyrano [c] chromene Derivatives Catalysed by Sodium Dodecyl Sulfate (SDS) in Neat Water. *J. Iran. Chem. Soc.* **2010**, *7*, 890–894. DOI: 10.1007/BF03246084.

[29] Parvanak Boroujeni, K.; Ghasemi, P. Synthesis and Application of a Novel Strong and Stable Supported Ionic Liquid Catalyst with Both Lewis and Brønsted Acid Sites. *Catal. Commun.* **2013**, *37*, 50–54. DOI: 10.1016/j.catcom.2013.03.025.

[30] Gupta, A. D.; Samanta, S.; Mondal, R.; Mallik, A. K. A Rapid, efficient and Green Method for Synthesis of 3,3'-arylmethylene-bis-4-hydroxycoumarins without Use of Any Solvent, catalyst or Solid Surface. *Chem. Sci. Trans.* **2013**, *2*, 524–528. DOI: 10.7598/cst2013.388.

[31] Al-Kadasi, A. M. A.; G. M. Ultrasound, N. Assisted Catalyst-free One-pot Synthesis of Biscoumarins in Neat Water. *Int. J. Chem. Sci* **2012**, *10*, 324–330.

[32] Parvanak Boroujeni, K.; Ghasemi, P.; Rafienia, Z. Synthesis of biscoumarin derivatives using poly 4-vinylpyridine, supported dual acidic ionic liquid as a heterogeneous catalyst. Monatsh. Chem. **2014**, 145, 1023–1026.

[33] Padalkar, V.; Phatangare, K.; Takale, S.; Pisal, R.; Chaskar, A. Silica Supported Sodium Hydrogen Sulfate and Indion 190 Resin: An Efficient and Heterogeneous Catalysts for Facile Synthesis of Bis-(4-hydroxycoumarin-3-yl) Methanes. *J. Saudi Chem. Soc.* **2015**, *19*, 42–45. DOI: 10.1016/j.jscs.2011.12.015.

[34] Zhu, A.; Bai, S.; Li, L.; Wang, M.; Wang, J. Choline Hydroxide: An Efficient and Biocompatible Basic Catalyst for the Synthesis of Biscoumarins under Mild Conditions. *Catal. Lett.* **2015**, *145*, 1089–1093. DOI: 10.1007/s10562-015-1487-6.

[35] Parvanak Boroujeni, K.; Hadizadeh, S.; Hasani, S.; Fadavi, A.; Shahrokh, M. Magnetite-containing Sulfonated Polyacrylamide as a Nanocatalyst for the Preparation of Biscoumarins. *Acta Chim Slov.* **2017**, *64*, 692–700. DOI: 10.17344/acsi.2017.3437.

[36] Patil, V. D.; Patil, K. P.; Sutar, N. R.; Gidh, P. V. Efficient Synthesis of Biscoumarins Using Zinc Acetate as a Catalyst in Aqueous Media. *Chem. Int.* **2017**, *3*, 240–243.

[37] Patil, S. K.; Awale, D. V.; Vadiyar, M. M.; Patil, S. A.; Bhise, S. C.; Kolekar, S. S. Simple Protic Ionic Liquid $[Et_3NH][HSO_4]$ as a Proficient Catalyst for Facile Synthesis of Biscoumarins. *Res. Chem. Intermed.* **2017**, *43*, 5365–5376. DOI: 10.1007/s11164-017-2932-5.

[38] Libor, Z.; Zhang, Q. The Synthesis of Nickel Nanoparticles with Controlled Morphology and SiO_2/Ni Core-shell Structures. *Mater. Chem. Phys.* **2009**, *114*, 902–907. DOI: 10.1016/j.matchemphys.2008.10.068.

[39] Kahani, S. A.; Shahrokh, M. Synthesis of $CuxNi_{1-x}$ Alloy Nanoparticles from Double Complex Salts and Investigation of Their Magnetoimpedance Effects. *RSC Adv.* **2015**, *5*, 71601–71607. DOI: 10.1039/C5RA09385F.

[40] Kahani, S. A.; Shahrokh, M. Preparation and Characterization of Cu–Co Alloy Nanoparticles from Double Complex Salts by Chemical Reduction. *New J. Chem.* **2015**, *39*, 7916–7922. DOI: 10.1039/C5NJ01441G.

[41] Kahani, S. A.; Mashhadian, F. Preparation of Bimetallic Co-Ag and Co-Cu Nanoparticles by Transmetallation of Tetrakis (pyridine)silver(II) peroxydisulfate and Tetrakis(pyridine) sulfatocopper(II) monohydrate Complexes. *J. Alloys* Compd. **2016**, *660*, 310–315. DOI: 10.1016/j.jallcom.2015.11.070.

[42] Parvanak Boroujeni, K.;Heidari, Z.; Khalifeh, R. Carbon Nanotube-supported Butyl 1-sulfonic Acid Groups as a Novel and Environmentally Compatible Catalyst for the Synthesis of 1,8-dioxo-Octahydroxanthenes. *Acta Chim Slov.* **2016**, 63, 602–608. DOI: 10.17344/acsi.2016.2291.

[43] Parvanak Boroujeni, K.; Tahani, P. The Cellulose Aluminum Oxide Composite-supported Imidazolium Chloroaluminate Ionic Liquid as a Novel and Stable Heterogeneous Catalyst. *Inorg. Nano-Met. Chem.* **2017**, *47*, 1150–1156. DOI: 10.1080/24701556.2017.1284103.

[44] Hwang, J.-H.; Dravid, V. P.; Teng, M. H.; Host, J. J.; Elliott, B. R.; Johnson, D. L.; Mason, T. O. Magnetic Properties of Graphitically Encapsulated Nickel Nanocatalyst. *J. Mater. Res.* **1997**, *12*, 1076–1082. DOI: 10.1557/JMR.1997.0150.

[45] Reller, L. B.; Weinstein, M.; Jorgensen, J. H.; Ferraro, M. J. Antimicrobial Susceptibility Testing: A Review of General Principles and Contemporary Practices. *Clin. Infect. Dis.* **2009**, *49*, 1749–1755. DOI: 10.1086/647952.

[46] Salganik, R. I. The Benefits and Hazards of Antioxidants: controlling Apoptosis and Other Protective Mechanisms in Cancer Patients and the Human Population. *J. Am. Coll. Nutr.* **2001**, *20*, 464S–472S.

[47] Duman, F.; Ocsoy, I.; Kup, F. O. Chamomile Flower Extract-directed CuO Nanoparticle Formation for Its Antioxidant and DNA Cleavage Properties. *Mater. Sci. Eng., C* **2016**, *60*, 333–338. DOI: 10.1016/j.msec.2015.11.052.

[48] Khanna, K. K.; Jackson, S. P. DNA Double-Strand Breaks: Signaling, Repair and the Cancer Connection. *Nat. Genet.* **2001**, *27*, 247–254. DOI: 10.1038/85798.